Diamond Detector Technology: Status and Perspectives

The RD42 Collaboration

A. Alexopoulos[3], M. Artuso[22], F. Bachmair[26], L. Bäni[26], M. Bartosik[3], J. Beacham[15], H. Beck[25], V. Bellini[2], V. Belyaev[14], B. Bentele[21], E. Berdermann[7], P. Bergonzo[13], A. Bes[30], J-M. Brom[9], M. Bruzzi[5], M. Cerv[3], G. Chiodini[29], D. Chren[20], V. Cindro[11], G. Claus[9], J. Collot[30], J. Cumalat[21], A. Dabrowski[3], R. D'Alessandro[5], D. Dauvergne[30], W. de Boer[12], C. Dorfer[26], M. Dünser[3], V. Eremin[8], R. Eusebi[27], G. Forcolin[24], J. Forneris[17], H. Frais-Kölbl[4], L. Gallin-Martel[30], M.L. Gallin-Martel[30], K.K. Gan[15], M. Gastal[3], C. Giroletti[19], M. Goffe[9], J. Goldstein[19], A. Golubev[10], A. Gorišek[11], E. Grigoriev[10], J. Grosse-Knetter[25], A. Grummer[23], B. Gui[15], M. Guthoff[3], I. Haughton[24], B. Hiti[11], D. Hits[26], M. Hoeferkamp[23], T. Hofmann[3], J. Hosslet[9], J-Y. Hostachy[30], F. Hügging[1], C. Hutton[19], H. Jansen[3], J. Janssen[1], H. Kagan[15], K. Kanxheri[31], G. Kasieczka[26], R. Kass[15], F. Kassel[12], M. Kis[7], V. Konovalov[15], G. Kramberger[11], S. Kuleshov[10], A. Lacoste[30], S. Lagomarsino[5], A. Lo Giudice[17], E. Lukosi[28], C. Maazouzi[9], I. Mandic[11], C. Mathieu[9], M. Menichelli[31], M. Mikuž,[11], A. Morozzi[31], J. Moss[15], R. Mountain[22], S. Murphy[24], M. Muš,kinja[11], A. Oh[24], P. Oliviero[17], D. Passeri[31], H. Pernegger[3], R. Perrino[29], F. Picollo[17], M. Pomorski[13], R. Potenza[2], A. Quadt[25], A. Re[17], M. Reichmann[*26], G. Riley[28], S. Roe[3], D. Sanz[26], M. Scaringella[5], D. Schaefer[3], C.J. Schmidt[7], S. Schnetzer[16], S. Sciortino[5], A. Scorzoni[31], S. Seidel[23], L. Servoli[31], S. Smith[15], B. Sopko[20], V. Sopko[20], S. Spagnolo[29], S. Spanier[28], K. Stenson[21], R. Stone[16], C. Sutera[2], B. Tannenwald[15], A. Taylor[23], M. Traeger[7], D. Tromson[13], W. Trischuk[18], C. Tuve[2], L. Uplegger[6], J. Velthuis[19], N. Venturi[18], E. Vittone[17], S. Wagner[21], R. Wallny[26], J.C. Wang[22], J. Weingarten[25], C. Weiss[3], T. Wengler[3], N. Wermes[1], M. Yamouni[30], and M. Zavrtanik[11]

[1]*Universität Bonn, Bonn, Germany*
[2]*INFN/University of Catania, Catania, Italy*
[3]*CERN, Geneva, Switzerland*
[4]*FWT, Wiener Neustadt, Austria*
[5]*INFN/University of Florence, Florence, Italy*
[6]*FNAL, Batavia, USA*
[7]*GSI, Darmstadt, Germany*
[8]*Ioffe Institute, St. Petersburg, Russia*
[9]*IPHC, Strasbourg, France*
[10]*ITEP, Moscow, Russia*
[11]*Jožef Stefan Institute, Ljubljana, Slovenia*
[12]*Universität Karlsruhe, Karlsruhe, Germany*

[13]*CEA-LIST Technologies Avancees, Saclay, France*
[14]*MEPHI Institute, Moscow, Russia*
[15]*The Ohio State University, Columbus, OH, USA*
[16]*Rutgers University, Piscataway, NJ, USA*
[17]*University of Torino, Torino, Italy*
[18]*University of Toronto, Toronto, ON, Canada*
[19]*University of Bristol, Bristol, UK*
[20]*Czech Technical University, Prague, Czech Republic*
[21]*University of Colorado, Boulder, CO, USA*
[22]*Syracuse University, Syracuse, NY, USA*
[23]*University of New Mexico, Albuquerque, NM, USA*
[24]*University of Manchester, Manchester, UK*
[25]*Universität Göttingen, Göttingen, Germany*
[26]*ETH Zürich, Zürich, Switzerland*
[27]*Texas A&M, College Park Station, TX, USA*
[28]*University of Tennessee, Knoxville, TN, USA*
[29]*INFN-Lecce, Lecce, Italy*
[30]*LPSC-Grenoble, Grenoble, France*
[31]*INFN-Perugia, Perugia, Italy*
[32]*California State University, Sacramento, CA, USA*
E-mail: `michael.reichmann@cern.ch`

The planned upgrade of the LHC to the High-Luminosity-LHC will push the luminosity limits even above the original design values. Since the current detectors will not be able to cope with this environment ATLAS and CMS are researching towards more radiation tolerant technologies for their innermost tracking layers. Chemical Vapour Deposition (CVD) diamond is an excellent candidate for this purpose. Detectors out of this material are already established in the highest irradiation regimes for the beam condition monitors at LHC. The RD42 collaboration is leading an effort to use CVD diamonds also as sensor material for the future tracking detectors. The signal behaviour of very high irradiated diamonds is presented as well as the recent study of the signal dependence on incident particle flux. There is also a recent development towards 3D detectors and especially 3D pixel detectors based on diamond sensors.

The European Physical Society Conference on High Energy Physics
5-12 July
Venice, Italy

---

*Speaker.

1. Introduction

The upgrade of the Large Hadron Collider (LHC) to the High-Luminosity-LHC (HL-LHC) from 2023 to 2025 [1] will push the luminosity limits even above the original design values of the LHC and will therefore hopefully give us even more insights in the fundamental nature of the universe. In 2028 an instantaneous luminosity of $5 \times 10^{34}\,\mathrm{cm^{-2}\,s^{-1}}$ is aspired. The innermost tracking layer at a distance of $\sim 30\,\mathrm{mm}$ will encounter pixel hit rates of $3\,\mathrm{GHz/cm^2}$ in this environment and is expected to be exposed to a total fluence of $2 \times 10^{16}\,\mathrm{n_{eq}/cm^2}$ in 2028 [2]. The current pixel detectors are designed to withstand $\sim 300\,\mathrm{fb^{-1}}$ and thus the full detector would have to be replaced about every year. This fact led to research and development of various radiation hard detector designs and materials.

Its large displacement energy of $42\,\mathrm{eV/atom}$ and a high band gap of $5.5\,\mathrm{eV}$ at $305\,\mathrm{K}$ make diamond an excellent candidate for such a radiation tolerant detector which is why the RD42 Collaboration is investigating single-crystal (sc) and poly-crystalline (p) Chemical Vapour Deposition (CVD) diamond as an alternative for precision tracking detectors for over two decades. In order to grow high quality detector grade diamonds, RD42 collaborates with industrial companies. All shown results are acquired with scCVD diamonds produced by Element Six Technologies [10] and pCVD diamonds produced by II-VI Incorporated [12]. The main difference between the two types are their sizes of $\sim 0.25\,\mathrm{cm^2}$ for scCVD and up to 6 inch for pCVD and the ⅔ smaller signal in pCVD [4]. In various studies it was shown that compared to corresponding silicon detectors, diamond is at minimum three times more radiation hard [8], has at least a two times faster charge collection [14] and its thermal conductivity is four times higher [17].

It is essential for all modern collider experiments to have an online monitoring of the beam conditions. Since it is important to have these detectors as close as possible to the beam all of the four main experiments at the LHC are using detectors with diamond sensors. ATLAS [11], ALICE, CMS [6] and LHCb [9] all make use of various Beam Condition Monitors (BCMs) and/or Beam Loss Monitors (BLMs) based on both CVD type diamonds for live background estimations and luminosity measurements.

Due to the very high particle fluxes and radiation doses expected for the HL-LHC it is very important to understand the behaviour of future detectors in this environment. The RD42 Collaboration has studied CVD diamond detectors with irradiation doses up to $2.2 \times 10^{16}\,\mathrm{p/cm^2}$. In order to build even more radiation hard detectors, a new technology - 3D detectors [3] - is investigated. The design of these detectors allows to heavily reduce the drift distance of the created charge carriers without reducing the total number of the created electron-hole pairs. Since the the signal behaviour of diamonds at high fluxes is uncertain, high rate studies are performed at Paul Scherrer Institut (PSI) with nearly minimum ionising particles (MIPs) and tunable particle fluxes from the order of $1\,\mathrm{kHz/cm^2}$ up to the order of $10\,\mathrm{MHz/cm^2}$.

2. CVD Diamond Detectors in the ATLAS Diamond Beam Monitor (DBM)

As an upgrade of the BCM during the long shutdown in 2014 ATLAS installed the DBM. Its purpose is to measure an instantaneous (bunch-by-bunch) luminosity and the bunch-by-bunch position of the beam spot. With its eight telescopes à three detector planes it adds tracking capability

to the existing precise time-of-flight (ToF) measurements of the eight pad detectors of the BCM. The usage of state of the art pixel detectors based on the FE-I4B readout chip (ROC) [5] strongly increases the spatial resolution of the monitor and due to its projective geometry pointing towards the interaction region it also can distinguish particles coming from collisions and background [7]. The telescopes, of which two are built from silicon and the other six from pCVD diamonds, are positioned symmetrically around the beam pipe on both sides of the interaction point (IP) and are shown in Figure 1. A total number of 45 diamonds with a thickness of 500 μm was available for the project of which 18 with the best quality were for chosen for the detector.

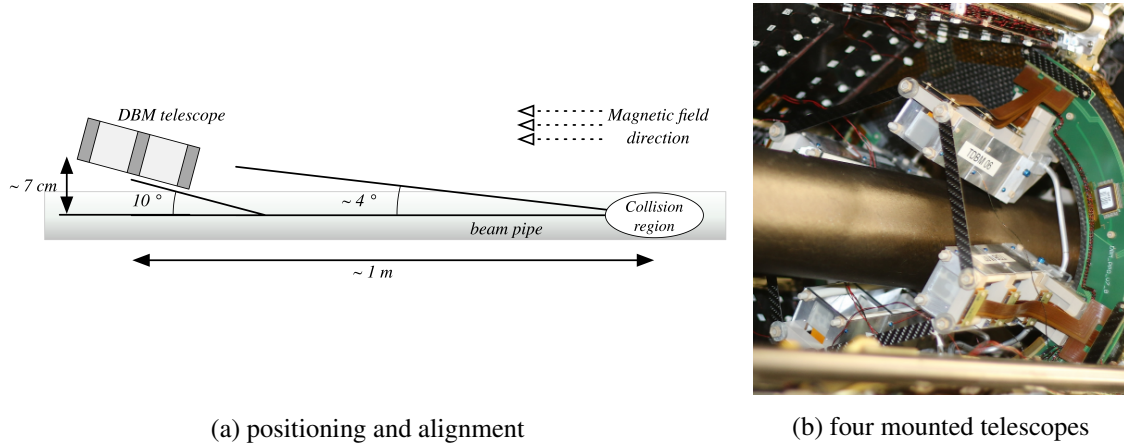(a) positioning and alignment

(b) four mounted telescopes

Figure 1: The positioning of DBM telescope around the beam pipe of the LHC

The first results already look promising and show a clear discrimination between collision and background events as demonstrated in Figure 2. During the shutdown of the LHC in the beginning of 2017 the modules were recommissioned and are a part of the ATLAS data taking now.
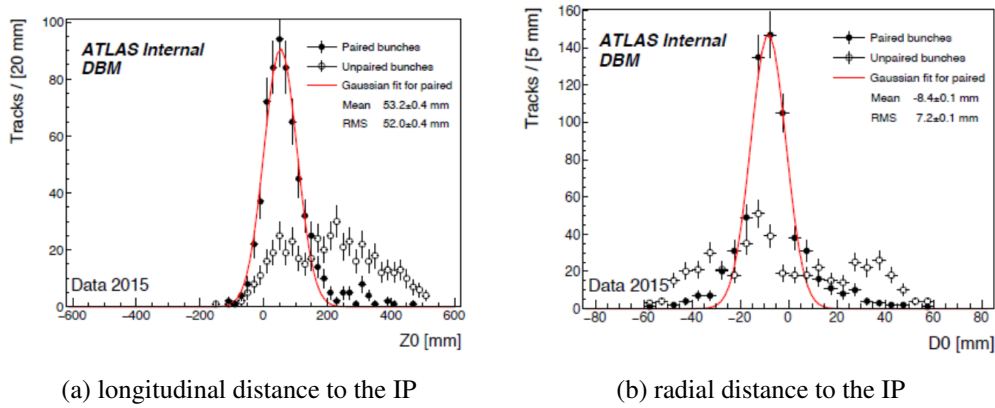

(a) longitudinal distance to the IP

(b) radial distance to the IP

Figure 2: Reconstruction of tracks from three modules using the initial alignment.

3. Radiation Tolerance

In order to probe the radiation tolerance of CVD diamond sensors several radiation studies have been performed varying the types and energies of damaging particles. The sensors were

2

irradiated with protons with energies of 24 GeV, 800 MeV, 70 MeV and 25 MeV, 1 MeV neutrons and 200 MeV pions up to a maximum dose of 2.2×10^{16} p/cm^2 which is equivalent to $\sim$500 Mrad. In order to built a detector out of a CVD diamond sensor a specific recipe is applied where the diamond gets metallised [15]. Depending on the geometry of the metallisation pattern, pad, strip and pixel detectors can be built. For the radiation studies a strip pattern was chosen in order to have a segmentation of the sensor.

3.1 Setup

The characterisation of the irradiated devices was performed at the Super Proton Synchrotron (SPS) beam line at CERN with charged hadrons with momenta of the order of 100 GeV/c. By using a customised beam telescope with a spacial resolution of $\sim$2 μm one obtains an unbiased hit prediction of the particle track in the diamond sensor. The schematic setup is shown in Figure 3.
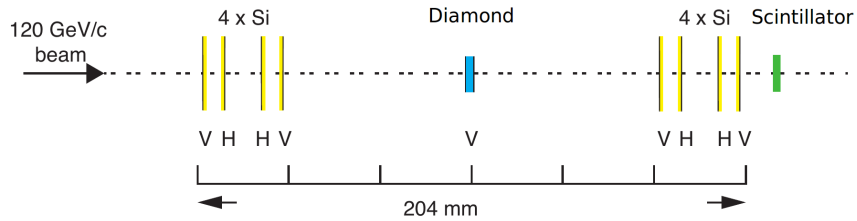

Figure 3: Schematic beam test setup consisting of two pairs of crossing silicon strip detectors on each side of the DUT and a scintillator in the end as reference.

3.2 Results

The signal behaviour of irradiated material follows the simple damage equation with the initial

$$\frac{1}{\lambda} = \frac{1}{\lambda_0} + \kappa\phi \qquad (3.1)$$

mean free path (MFP) λ_0, the damage constant κ and the fluence ϕ. Since the measurable quantity is the charge collection distance (CCD) we have to use a model to find a relation to the mean free path [4].

The results of two different types of irradiation are shown in Figure 4 on the next page. As seen in the examples all of the tested samples follow the equation 3.1. Table 1 on the next page shows all the extracted damage constants. As expected neutrons and low energy protons create the biggest damage in the material.

4. High Rate Beam Tests

In addition to the radiation studies it is also very important to understand the signal behaviour of CVD diamonds depending on the incident particle flux since the HL-LHC will reach values in the low GHz/cm^2 range. In order to conduct such a study it is important to have the possibility to vary the particle flux in big range. The πM1 beam line at the High Intensity Proton Accelerator (HIPA)
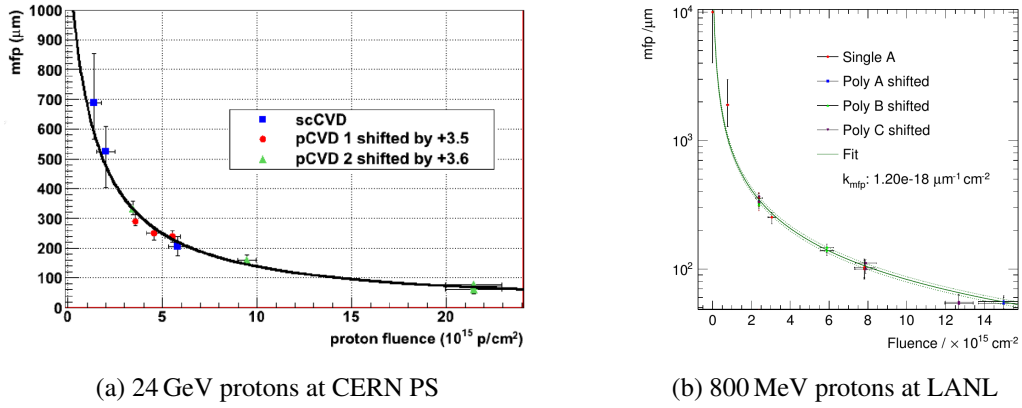
(a) 24 GeV protons at CERN PS

(b) 800 MeV protons at LANL

Figure 4: Irradiation results

Particle	Energy	Relative κ
Proton	24 GeV	1.0
	800 MeV	1.79 ± 0.13
	70 MeV	2.4 ± 0.4
	25 MeV	4.5 ± 0.6
Neutron	1 MeV	4.5 ± 0.5
Pion	200 MeV	$2.5 - 3$

Table 1: Damage constants for various irradiation types normalised to 24 GeV protons

at PSI can provide beams with continuously tunable fluxes from the order of $1 \, \text{kHz/cm}^2$ up to $10 \, \text{MHz/cm}^2$ which have a spacing of $19.8 \, \text{ns}$ between each bunch. For these studies a π^+ beam with with a momentum of $260 \, \text{MeV/c}$ was chosen in order to reach the highest possible flux.

The diamond sensors were measured in a pad geometry and prepared in the same fashion described in [16]. In order to resolve single waveforms at high particle rates the sensors are hooked up to a fast, low-noise amplifier with a rise time of approximately $5 \, \text{ns}$. The resulting waveforms are then read out with a DRS4 Evaluation Board at a sampling frequency of $2 \, \text{GHz}$. The final diamond pad detectors are then brought into a beam telescope based on the CMS pixel ROCs PSI46v2 [13] which provides precise tracking with a resolution of $\sim 70 \, \mu\text{m}$ as well as a trigger which can be scaled in area to increase the efficiency of the data taking. At the end

Figure 5: Rate Setup

of the telescope sits a scintillator as additional trigger to achieve a precise timing of $1 \, \text{ns}$. The full setup is shown in Figure 5.
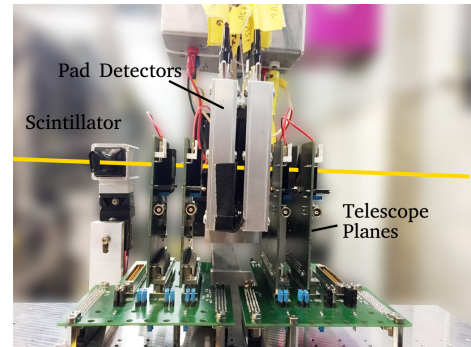
An overlay of 30000 resulting waveforms is shown in Figure 6 on the next page. The most frequent peak at $70 \, \text{ns}$ relates to the actual particle which was triggered on and is called signal region. All the other peak are secondary particles from other bunches. Due to the good timing resolution the bunch spacing of the PSI beam can be clearly seen in the plot. The bunch just before the signal

region is forbidden by the trigger logic. Therefore there are no peaks in this area and it is used to extract the pedestal (base line) of the waveform. The pulse height value is then calculated by the an integral with a range of 4 ns before and 6 ns after the maximum value in the signal region. The optimisation of the integration window was done by choosing the best Signal to Noise Ratio (SNR).
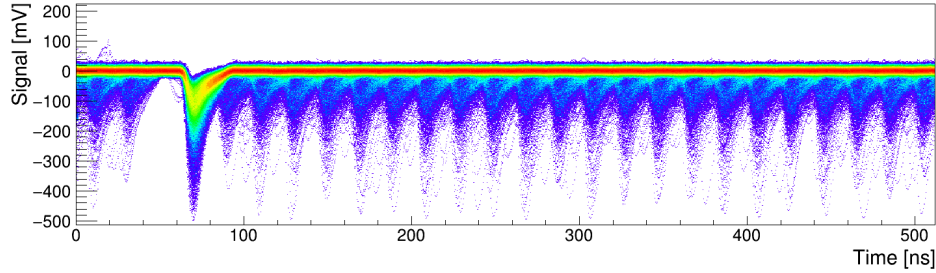

Figure 6: 30000 pCVD diamond waveforms

In order to check the dependence on the incident particle flux several rate scans with both bias voltages and different irradiation doses were performed. The typical scan was starting at the minimum flux, going up to maximum flux with 4 to 5 steps in between (up scan) and then going down to the minimum flux again (down scan). Several of the up and down scans were done in succession to check for long time effects. Figure 7 shows the final results for a pCVD diamond both non-irradiated and irradiated to $5 \times 10^{14} \, \text{n}_{\text{eq}}/\text{cm}^2$. As shown, no pulse height dependence on particle flux was observed for a flux up to $10 \, \text{MHz}/\text{cm}^2$. In addition it can also be seen that there is a slight difference between positive and negative bias. After the irradiation the pulse decreases due to the radiation damage but the values have no absolute calibration yet.
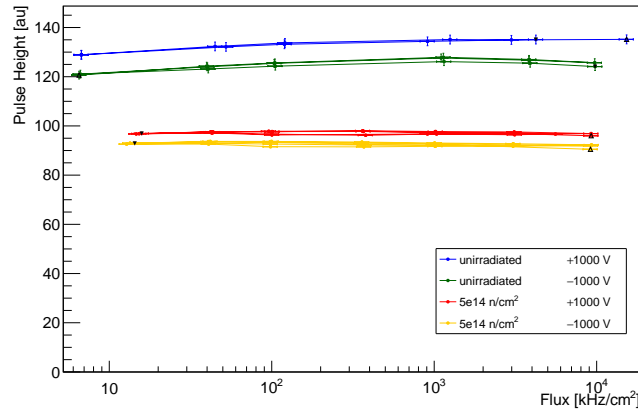

Figure 7: Pulse height versus incident particle flux for a pCVD diamond

5. 3D Detectors

The radiation damage created by HL-LHC will become a big challenge for the innermost tracking detectors. After a large irradiation, all detector material will become trap limited with a

5

MFP below 75 μm. The concept of a so called 3D-Detector is a possible way to highly increase the longevity of these materials. More details about the fabrication and the functionality can be found in [3].

In 2015 one of the first detectors was built out of a pCVD diamond sensor which had a 3D detector as well as a strip detector on the same sensor. At this time the column efficiency was about 92 % and the 3D cells had a size of 150 μm × 150 μm. This detector was already a success by showing a working 3D diamond detector. Its square cells are clearly visible and the measured signal for the thickness of 500 μm was 13 500 e which is much higher than 6900 e in the strip detector. The strip signal equates to a CCD of 192 μm. The measured charge in the 3D would have a CCD in a planar detector of 350 μm to 375 μm which effectively means that more than 75 % of the created charge was collected for the first time in a pCVD diamond. The according pulse height distributions are shown in figure 8. The next step followed in 2016 when the full 3D detectors was built was dramatic improvements. The number of cells

Figure 8: Pulse height of the 3D multi detector

went up from 99 to 1188, the cell size was reduced to to 100 μm × 100 μm and the column efficiency could be increased to 99 %. The analysis of this device is still in progress but the first results already look very promising. There is charge in the entire area of the detector and we see the largest charge collection in pCVD yet with over 85 % in a contiguous region.

Finally in the end of 2016 the first pCVD 3D pixel detector was built. A 3D diamond sensor was metallised and then bump bonded to a CMS pixel ROC PSI46digV2.1respin [13]. The chip was then tuned to a global pixel threshold of 1500 e. The preliminary beam test results already look very with an efficiency of 98.5 %. This value is close to the efficiency of the silicon pixel of 99.3 % which was tested in parallel. The slightly lower value is believed to origin from the low field regions between the electrodes.
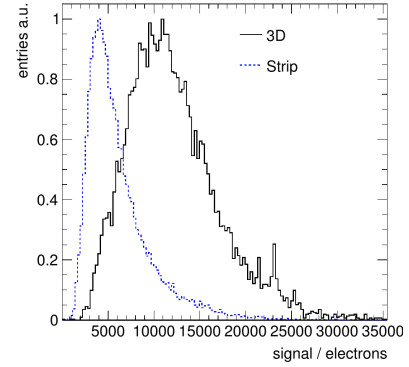
6. Conclusion

By now the technology of diamond detectors is well established in high energy physics. Many of the experiments are already using BCMs or BLMs based on diamonds and their impact is steadily increasing. As one of the first pixel projects the ATLAS DBM started taking data and was recommissioned for the 13 TeV collisions.

The diamond material was proven to be very radiation hard and the signal behaviour after the irradiation with various particle species and energies is very well understood for both scCVD and pCVD diamonds. In extensive studies it was also found out that pCVD diamond detectors work reliably and show no signal dependence up to an incident particle flux of 10 MHz/cm^2. This could also be shown for irradiated detectors up to fluence of 5×10^{14} n$_{eq}$/cm^2.

There is also great progress in the development of even more radiation hard devices. The working principle of both 3D strip and pixel detectors could be proven with great success down to cell sizes of 100 μm × 100 μm. For the first time more than 80 % of the created charge in the material could

be read out. The efficiency of the column drilling process is now above 99 % and the total efficiency of the 3D pixel detectors is very high with 98.5 %.

References

[1] G Apollinari, I Béjar Alonso, O Brüning, M Lamont, and L Rossi. *High-Luminosity Large Hadron Collider (HL-LHC): Preliminary Design Report*. CERN Yellow Reports: Monographs. CERN, Geneva, 2015.

[2] Georg Auzinger. Upgrade of the CMS Tracker for the High Luminosity LHC. Technical Report CMS-CR-2016-268, CERN, Geneva, Oct 2016.

[3] F. Bachmair, L. Bäni, P. Bergonzo, B. Caylar, G. Forcolin, I. Haughton, D. Hits, H. Kagan, R. Kass, L. Li, A. Oh, S. Phan, M. Pomorski, D.S. Smith, V. Tyzhnevyi, R. Wallny, and D. Whitehead. A 3d diamond detector for particle tracking. *Nuclear Instruments and Methods in Physics Research Section A: Accelerators, Spectrometers, Detectors and Associated Equipment*, 786:97 – 104, 2015.

[4] Felix Caspar Bachmair. *CVD Diamond Sensors In Detectors For High Energy Physics*. PhD thesis, Zurich, ETH, 2016.

[5] M Backhaus. Characterization of the FE-I4B pixel readout chip production run for the ATLAS Insertable B-layer upgrade. *JINST*, 8(AIDA-PUB-2013-020):C03013, Mar 2013.

[6] E. Bartz, J. Doroshenko, V. Halyo, B. Harrop, D.A. Hits, D. Marlow, L. Perera, S. Schnetzer, and R. Stone. The plt: A luminosity monitor for cms based on single-crystal diamond pixel sensors. *Nuclear Physics B - Proceedings Supplements*, 197(1):171 – 174, 2009. 11th Topical Seminar on Innovative Particle and Radiation Detectors (IPRD08).

[7] Matevz Cerv. The atlas diamond beam monitor. 9:C02026, 02 2014.

[8] Wim de Boer, Johannes Bol, Alex Furgeri, Steffen Müller, Christian Sander, Eleni Berdermann, Michal Pomorski, and Mika Huhtinen. Radiation hardness of diamond and silicon sensors compared. *physica status solidi (a)*, 204(9):3004–3010, 2007.

[9] M. Domke, C. Ilgner, S. Kostner, M. Lieng, M. Nedos, J. Sauerbrey, S. Schleich, B. Spaan, and K. Warda. Commissioning of the beam conditions monitor of the lhcb experiment at cern. In *2008 IEEE Nuclear Science Symposium Conference Record*, pages 3306–3307, Oct 2008.

[10] elementsix - industry leading engineers. `https://e6cvd.com`, 2017.

[11] A. Gorišek, V. Cindro, I. Dolenc, H. Frais-Kölbl, E. Griesmayer, H. Kagan, S. Korpar, G. Kramberger, I. Mandi, M. Meyer, M. Miku, H. Pernegger, S. Smith, W. Trischuk, P. Weilhammer, and M. Zavrtanik. Atlas diamond beam condition monitor. *Nuclear Instruments and Methods in Physics Research Section A: Accelerators, Spectrometers, Detectors and Associated Equipment*, 572(1):67 – 69, 2007. Frontier Detectors for Frontier Physics.

[12] Ii-vi incorporated : A global leader in engineered materials and optoelectronic devices and components. `http://www.ii-vi.com/`, 2017.

[13] Andreas Kornmayer, Thomas Müller, and Ulrich Husemann. Studies on the response behaviour of pixel detector prototypes at high collision rates for the CMS experiment, Nov 2015. Presented 04 Dec 2015.

[14] H Pernegger, V Eremin, H Frais-Kölbl, E Griesmayer, H Kagan, S Roe, S Schnetzer, R Stone, W Trischuk, D Twitchen, Peter Weilhammer, and A Whitehead. Charge-carrier properties in synthetic single-crystal diamond measured with the transient-current technique. *J. Appl. Phys.*, 97(7):73704–1–9, 2005.

[15] Ricardo S. Sussmann. *CVD diamond for electronic devices and sensors*. John Wiley & Sons, Chichester, 2009.

[16] R Wallny. Beam test results of the dependence of signal size on incident particle flux in diamond pixel and pad detectors. *JINST*, 10(07):C07009, 2015.

[17] Shu-lai Zhao. *Characterization of the electrical properties of polycrystalline diamond films*. PhD thesis, Ohio State U., 1994.